The FEBS Journal

FEBS PRESS science publishing by scientists

Structures of a diverse set of colchicine binding site inhibitors in complex with tubulin provide a rationale for drug discovery

Yuxi Wang[1,*], Hang Zhang[1,*], Benoît Gigant[2], Yamei Yu[1], Yangping Wu[1], Xiangzheng Chen[1], Qinhuai Lai[1], Zhaoya Yang[3], Qiang Chen[1] and Jinliang Yang[1]

1 State Key Laboratory of Biotherapy and Cancer Center, West China Hospital, Collaborative Innovation Center for Biotherapy, Sichuan University, Chengdu, China
2 Institute for Integrative Biology of the Cell (I2BC), CEA, CNRS, Université Paris-Sud, Gif-sur-Yvette, France
3 West China School of Pharmacy, Sichuan University, Chengdu, China

Keywords
colchicine binding domain; crystal structure; drug design; pharmacophore; tubulin inhibitor

Correspondence
Q. Chen or J. Yang, State Key Laboratory of Biotherapy and Cancer Center, West China Hospital, Sichuan University, and Collaborative Innovation Center for Biotherapy, Chengdu 610041, China
Fax: +86 28 85164060; +86 28 85502796;
Tel: +86 28 62336597; +86 28 85502796
E-mails: qiang_chen@scu.edu.cn; jinliangyang@scu.edu.cn

*These authors contributed equally to this work

(Received 18 August 2015, revised 22 September 2015, accepted 9 October 2015)

doi:10.1111/febs.13555

Microtubules are dynamic assemblies of αβ-tubulin heterodimers and have been recognized as highly attractive targets for cancer chemotherapy. A broad range of agents bind to tubulin and interfere with microtubule assembly. Despite having a long history of characterization, colchicine binding site inhibitors (CBSIs) have not yet reached the commercial phase as anti-cancer drugs to date. We determined the structures of tubulin complexed with a set of structurally diverse CBSIs (lexibulin, nocodazole, plinabulin and tivantinib), among which nocodazole and tivantinib are both binary-function inhibitors targeting cancer-related kinases and microtubules simultaneously. High resolution structures revealed the detailed interactions between these ligands and tubulin. Our results showed that the binding modes of the CBSIs were different from previous docking models, highlighting the importance of crystal structure information in structure-based drug design. A real structure-based pharmacophore was proposed to rationalize key common interactions of the CBSIs at the colchicine domain. Our studies provide a solid structural basis for developing new anti-cancer agents for the colchicine binding site.

Database
The atomic coordinates and structure factors for tubulin complexed with lexibulin, nocodazole, plinabulin and tivantinib have been deposited in the Protein Data Bank under accession codes 5CA0, 5CA1, 5C8Y and 5CB4, respectively.

Introduction

As a major component of the eukaryotic cell cytoskeleton, microtubules play a crucial role in many cellular events and have been recognized as highly attractive targets for cancer chemotherapy [1,2]. Microtubules are made of αβ-tubulin heterodimers that assemble into protofilaments in a head-to-tail fashion, and the straight and parallel protofilaments interact laterally to form the microtubule hollow cylinder [3]. A wide range of small molecules bind to tubulin and interfere with microtubule dynamics. Subsequent to the approval of vincristine by the FDA in 1963[4], research on tubulin targeting agents has

Abbreviations
ABC-transporter, ATP-binding cassette transporter; CBSI, colchicine binding site inhibitor; PDB, Protein Data Bank; TTL, tubulin tyrosine ligase; VDA, vascular disrupting agent.

remained active for cancer treatment. Five binding sites for exogenous agents on tubulin have been identified, namely the taxane [5], vinca alkaloid [6], colchicine [7], laulimalide [8] and maytansine [9] domains. Most anti-microtubule drugs in development target one of these binding sites. Among the different types of anti-tubulin agents, colchicine binding site inhibitors (CBSIs) have the longest history of research, although they have not yet reached the commercial phase to date for the treatment of cancers [10].

Colchicine was initially isolated from the leaves of meadow saffron (*Colchicum autumnale*) to treat gout [11]. Its physiological target was identified as tubulin in 1968 [12]. The structures of colchicine and of several CBSIs bound to tubulin have been determined, and the inhibition mechanism of microtubule assembly has been revealed [7,13–15]. These compounds target the β subunit of curved (unassembled) tubulin and prevent it from adopting a straight (microtubular) structure either by steric clashes with the α subunit [7] or by preventing the tubulin subdomain movements that occur during the curved-to-straight structural conversion [13]. A hallmark of the CBSIs is that they comprise a large group of structurally diverse natural and synthetic compounds that target different tubulin binding subsites. Therefore, it is difficult to determine their interactions with tubulin by computer modeling. Experimental approaches are still needed in that respect.

In the present study, we chose a set of structurally diverse CBSIs (lexibulin, nocodazole, plinabulin and tivantinib) and determined their structures in complex with tubulin to high resolutions (2.2–2.6 Å). Interestingly, among these ligands, nocodazole and tivantinib are both binary-function inhibitors targeting both cancer-related kinases and microtubules. Structural analysis revealed the detailed interactions between these ligands and tubulin, and underlined the importance of the crystal structure in structure-based drug design. We propose a real structure-based pharmacophore for rationalizing key common interactions of the CBSIs at the colchicine domain. Our studies provide a solid structural basis for the development of new anti-cancer agents targeting the colchicine binding site.

Results

In the present study, we chose four CBSIs that are structurally diverse colchicine site compounds (Fig. 1C). We solved the crystal structure of tubulin–ligand complexes to obtain insights into the binding mode of these compounds. Structures were determined to resolutions ranging from 2.2 to 2.6 Å. Details of the data collection and refinement statistics are summarized in Table 1.

As expected, all four CBSIs bound to the colchicine binding site (Fig. 1A,B). Comparison between different complex structures, including the tubulin–colchicine

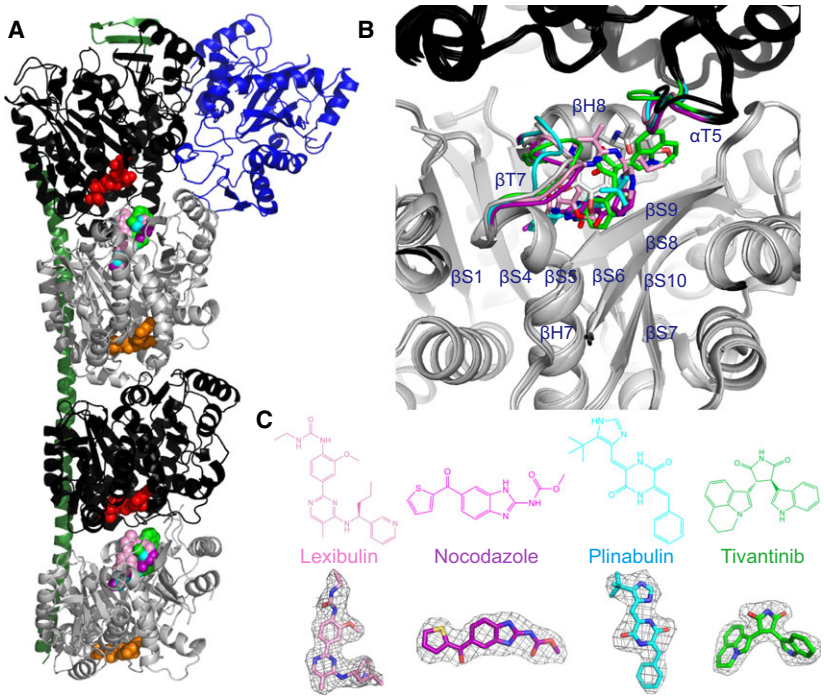

Fig. 1. Structures of CBSIs complexed with tubulin. (A) Overall structure of the CBSI–tubulin complex. The RB3–SLD is colored green, TTL is blue, α-tubulin is black, β-tubulin is grey, GTP is red and GDP is orange. The CBSIs are superimposed and colored as in (C). (B) The CBSI binding site. The colchicine–tubulin structure (PDB code: 4O2B) and the four CBSI–tubulin complexes are superimposed. The CBSIs and two loops (αT5 and βT7) are colored as in (C). For the colchicine–tubulin structure, colchicine is colored in grey, α-tubulin is black and β-tubulin is grey. (C) Chemical formulas and electron densities of the four CBSIs used in the present study. The $F_o - F_c$ omit maps are contoured at 3 σ.

Table 1. Crystallographic data and structure refinement statistics.

Ligand	Lexibulin	Nocodazole	Plinabulin	Tivantinib
Data collection				
X-ray source	BL19U1	BL19U1	BL17U1	BL19U1
Wavelength (Å)	0.97853	0.97853	0.97915	0.97853
Resolution range (Å)	50–2.5 (2.54–2.50)[a]	50–2.4 (2.44–2.40)	50–2.6 (2.69–2.60)	50–2.2 (2.24–2.20)
Space group	$P\,2_12_12_1$	$P\,2_12_12_1$	$P\,2_12_12_1$	$P\,2_12_12_1$
Unit cell (*a*, *b*, *c*) (Å)	105.6, 158.4, 181.8	105.4, 158.4, 180.7	105.4, 157.6, 182.4	105.3, 158.5, 181.4
Total reflections	703 565	807 753	396 168	1 050 210
Unique reflections	104 340	118 147	93 390	154 428
Multiplicity	6.7 (6.9)	6.8 (7.1)	4.2 (4.1)	6.8 (6.4)
Completeness (%)	100 (100)	100 (100)	99.8 (99.7)	100 (99.3)
Mean $I/\sigma(I)$	15.5 (2.0)	12.9 (2.5)	11.6 (2.1)	18.7 (2.6)
R_{merge}	0.150 (0.847)	0.116 (0.632)	0.121 (0.826)	0.103 (0.525)
Refinement				
R_{factor}/R_{free}[b]	0.208/0.235	0.193/0.237	0.197/0.245	0.210/0.240
rmsd (bond)	0.007	0.005	0.003	0.008
rmsd (angle)	1.10	1.02	0.69	1.57
Number of atoms				
Proteins	17 256	17 267	17 267	17 267
Ligands	238	228	218	230
Waters	171	377	262	830
Average B-factor				
Proteins	65.10	42.60	53.60	46.10
Ligands	62.74	32.89	58.50	32.86
Waters	58.50	36.30	46.80	43.40
Ramachandran plot statistics				
Most favored (%)	91.3	91.0	90.9	92.6
Allowed (%)	8.6	8.9	8.9	7.3
Generously allowed (%)	0.1	0.1	0.2	0.1
Disallowed (%)	0	0	0	0

[a] The values for the data in the highest resolution shell are shown in parentheses.

[b] $R_{free} = \sum \text{Test} ||F_{obs}| - |F_{calc}|| / \sum \text{Test} |F_{obs}|$, where 'Test' is a test set of approximately 5% of the total reflections randomly chosen and set aside prior to refinement for the structure.

complex, showed that the binding of the different colchicine-site ligands did not affect the global conformation of tubulin, nor of the T2R complex. The rmsd for approximately 2000 Cα atoms is less than 0.5 Å for all pairwise comparisons of tubulin–ligand complexes. The major conformational changes involve two loops near the colchicine binding site, βT7 and αT5 (Fig. 1B). The nomenclature of tubulin secondary structure elements and loops is provided in Löwe *et al*. [16].

The high resolutions and clear density maps enabled us to determine the positions and orientations of the small-molecule inhibitors unambiguously (Fig. 1C), thus revealing the detailed interactions between these agents and tubulin (Fig. 2).

Colchicine targets the β subunit of curved tubulin and prevents it to adopt a straight structure. This likely accounts for the inhibition of microtubule assembly [7,13]. Consistent with these previous reports, the binding of the CBSIs investigated in the present study also hindered the curve-to-straight transition of tubulin by the steric clashes between the CBSIs and surrounding secondary structure elements (Fig. 3). Thus, these CBSIs likely share the same inhibition mechanism as that of colchicine.

Lexibulin binding

Lexibulin is a microtubule polymerization inhibitor which is under phase II clinical trials for the treatment of glioblastoma multiforme and relapsed and refractory multiple myeloma [17–19]. In the tubulin–lexibulin complex structure, lexibulin occupied a position partially overlapping with that of colchicine, and made hydrogen bonds with the main chain of βV236 on H7, βD249 on T7 and αT179 on T5 (Fig. 2A).

During the discovery of lexibulin, a series of analogue compounds have been synthesized and evaluated [20]. Chain elongation of the benzylic carbon alkyl substituent led to a significant increase in cellular activity, which may be a result of the accommodation

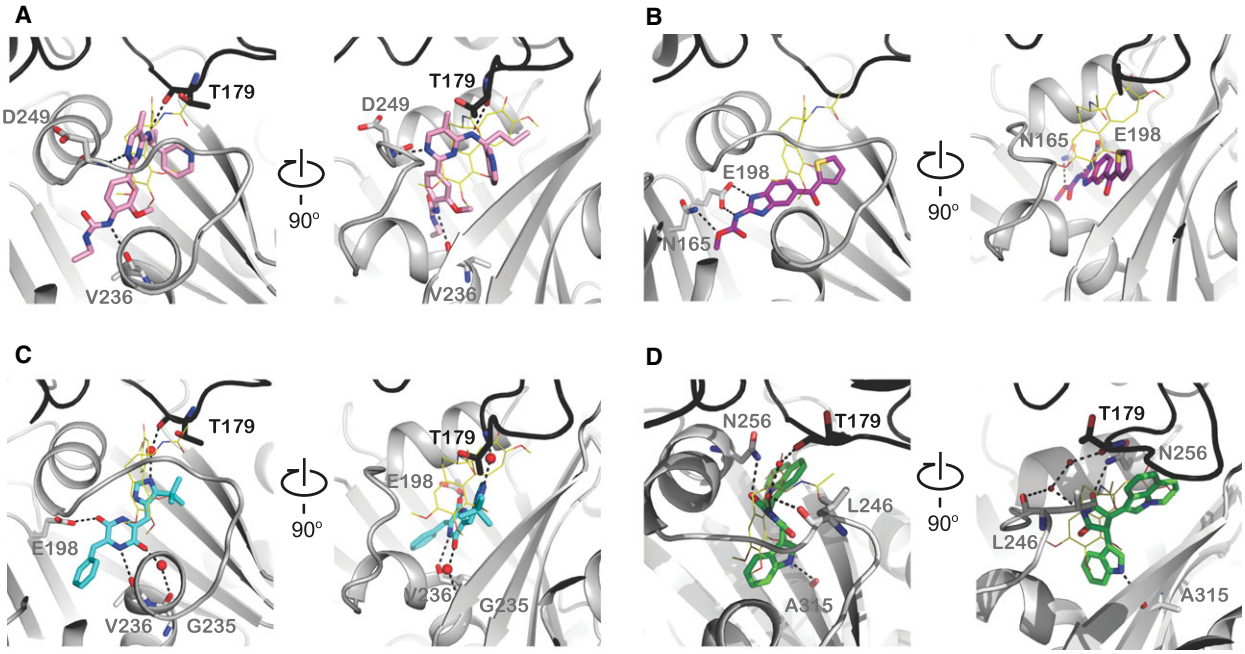

Fig. 2. Interactions between CBSIs and tubulin. Tubulin and CBSIs are colored as in Figure 1. For comparison, colchicine (PDB code: 4O2B) is shown in yellow in each case. CBSIs are shown as sticks: (A) lexibulin, (B) nocodazole, (C) plinabulin and (D) tivantinib. Residues that make hydrogen bonds with the CBSIs are shown as sticks and are labeled.

of the longer chain in a hydrophobic pocket. By contrast, substitutions at position 4 of the benzylic aryl ring reduce the potency of the compound, most likely because the substituted group results in steric hindrance with βS9 (Fig. 4A).

Nocodazole binding

Nocodazole is a high-affinity ligand for the cancer-related kinases ABL, c-KIT, BRAF and MEK [21] and a rapidly-reversible inhibitor of microtubule polymerization [22]. Different nocodazole–tubulin binding models have been proposed. In one of them, nocodazole occupies a position similar to colchicine [23]. More recently, a docking model based on drug resistance associated mutations has placed nocodazole much deeper in the β subunit [24]. Our crystal structure data agree with the later. Nocodazole did not interact with the α subunit but made hydrogen bonds with βN165 on S5 and βE198 on S6, and overlapped very little with colchicine (Fig. 2B). A previously reported CBSI, TN16, occupied a very similar position as nocodazole [13] (Fig. 5).

Tubulin exists as various isotypes in mammalian cells with different distribution and drug-binding properties [25]. Nocodazole has a three- to five-fold lower affinity for the αβIII isotype compared to that of the αβII and αβIV ones [26]. We found that cysteine β239 on H7 positioned its sulfhydryl group close to nocodazole (closest distance between the sulfur atom and a nocodazole oxygen atom: 3.9 Å) (Fig. 4B). Although residue 239 is a cysteine in the βII and βIV isotype, in βIII tubulin, a serine residue is found at this position. Compared to the sulfhydryl group, the hydroxyl group is smaller in size and has a greater polarity, which may be unfavorable for nocodazole binding.

Plinabulin binding

Plinabulin is a vascular disrupting agent (VDA) with microtubule depolymerizing activity and is under phase I/II clinical trials for treatment of cancers [27,28]. Previous studies have suggested that the plinabulin binding site is in the boundary region of tubulin heterodimer interface, and not inside the colchicine binding cavity [29]. However, the tubulin–plinabulin complex structure showed just the opposite: plinabulin resided in a deeper position in β-tubulin, making hydrogen bonds with βE198 on S6 and βV236 on H7, and also interacting with βG235 on H7 and with αT179 on T5 via water molecules (Fig. 2C). Our structure showed little overlap between plinabulin and colchicine.

Tivantinib binding

Tivantinib is the first non-ATP-competitive c-Met inhibitor undergoing phase I/II/III clinical trials for the

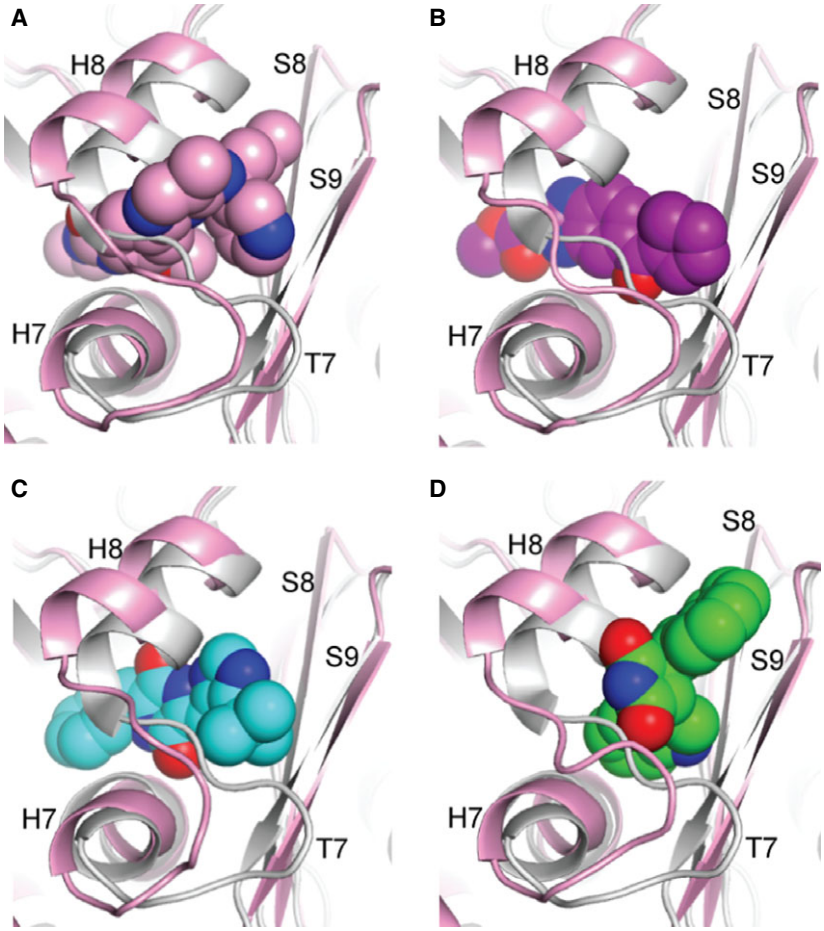

Fig. 3. Interference of CSBIs with the tubulin straight conformation. Superimposition of the tubulin–ligand complexes (salmon) and tubulin as found in straight protofilaments (PDB code: 1JFF; gray) reveals that CBSI binding is not compatible with the straight conformation. The ligand molecules are shown in sphere representation: (A) lexibulin, (B) nocodazole, (C) plinabulin and (D) tivantinib. Regions of steric clashes between straight tubulin and ligands are labeled (S8, S9, H7, T7 and H8).

treatment of cancers [30–32]. A recent study demonstrated that tivantinib directly bound to the colchicine binding site of tubulin to exhibit anti-tumor activity and could overcome ABC transporter-mediated multidrug resistance [33]. To clarify the binding mode and inhibition mechanism of tivantinib to tubulin, we determined the crystal structure of the tubulin–tivantinib complex, and found the tivantinib binding site had a large overlap with that of colchicine (Fig. 2D). Tivantinib made hydrogen bonds with βN256 on H8 and βA315 on S8, and also interacted with βL246 on T7 and αT179 on T5 via water molecules (Fig. 2D). The tivantinib binding site in a previous docking model is very similar to that in the crystal structure, although the orientation of tivantinib is reversed [33].

Pharmacophore for the colchicine domain

A 'colchicine domain' made of a main site and of additional extensions has been proposed [13]. Our results permit us to refine the colchicine domain definition. The colchicine domain is a big pocket surrounded

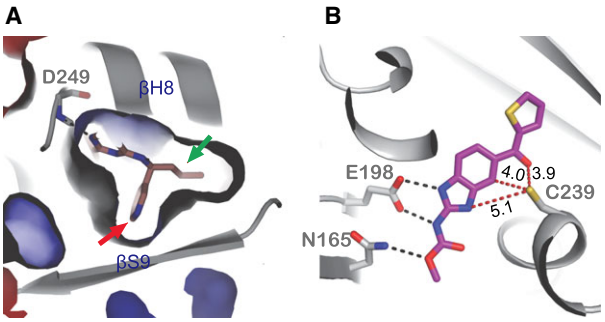

Fig. 4. The microenvironment at the colchicine domain affects ligand binding affinity. (A) A cutaway view showing the binding pocket around the lexibulin benzylic aryl ring. The green arrow indicates the benzylic carbon alkyl substituent, a propyl group, which fits well with the hydrophobic pocket. The red arrow indicates the atom C4 of the benzylic aryl ring, with substitutions at this position tending to conflict with βS9. (B) The sulfhydryl group of βC239 side-chain is close to the bound nocodazole. The residue βC239 and two other residues involved in nocodazole binding are shown as sticks and labeled. Molecules are colored as in Fig. 1. Hydrogen bonds and distances (Å) are indicated by black and red dashed lines, respectively.

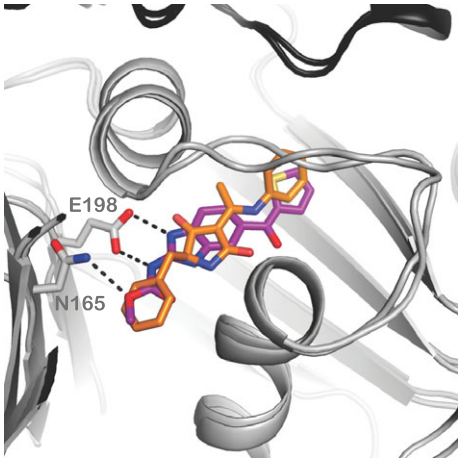

Fig. 5. Superposition of the structures of tubulin–nocodazole and tubulin–TN16. Nocodazole is colored purple, TN16 is orange, α-tubulin is black and β-tubulin is grey. Residues that form hydrogen bonds with nocodazole are shown as sticks and are labeled.

by two α-helices (H7 and H8) and by strands of the two tubulin β-sheets (S1-S4-S5-S6 and S7-S10-S8-S9) from the β subunit and is capped by two loops (βT7 and αT5) (Fig. 6A). It is noteworthy that βS7 paired with both βS6 and βS10 via its N-terminus and C-terminus, respectively, thus bridging the two β-sheets into a super β-sheet.

A pharmacophore model has been proposed to summarize the CBSIs interactions at the colchicine domain [23]. However, the docking-model-based pharmacophore limited its accuracy and rationality for drug discovery. Here, we collected previously determined CBSI–tubulin crystal structures in addition to the four structures reported in the present study to construct a real structure-based pharmacophore for rationalizing key common interactions of the CBSIs at the colchicine domain (Fig. 6).

We propose a pharmacophore consisting of five points: three hydrophobic centers (I, II and III) and two hydrogen bond centers (IV and V, either hydrogen bond acceptor or donor) (Fig. 6B). The point II is a major hydrophobic group represented in all these CBSIs, fitting the hydrophobic core of the colchicine domain. Two extended hydrophobic pockets in the colchicine domain accommodate two other hydrophobic groups: one is buried deeply in β-tubulin (point I) and the other one is located at the interface of the α/β tubulin heterodimer (point III). The hydrophilic groups (points IV and V) may form hydrogen bonds with tubulin (Fig. 6B).

Discussion

We have chosen an atypical set of CBSIs that is structurally diverse. Docking models for interactions with tubulin have been proposed for three of the four CBSIs reported in the present study. In the case of nocodazole, different models have been proposed [23,24]. In the case of plinabulin, the modeling has placed it in a position that largely overlaps colchicine [29]. By contrast, our crystal structures showed that the binding site of plinabulin, as well as that of

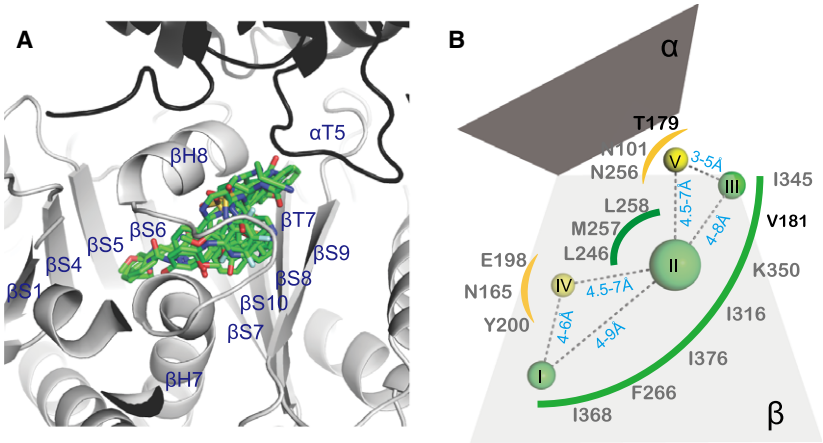

Fig. 6. Pharmacophore model for CBSIs. (A) Superposition of CBSIs whose structure with tubulin has been determined. The four CBSIs reported in the present study and five reported previously (PDB code: 4O2A, 4O2B, 3HKC, 3HKD and 3HKE) are superimposed. Their carbon atoms are colored green, nitrogen atoms are blue, oxygen atoms are red, sulfur atoms are yellow and chlorine atoms are cyan. (B) Schematic drawing of the common pharmacophore for ligand binding to the colchicine domain. The hydrophobic and hydrophilic centers are shown as green and yellow balls, respectively. The residues potentially involved are labeled black for the residues from α-tubulin and grey for those from β-tubulin.

nocodazole, had little overlap with that of colchicine (Fig. 2B,C). In the docking model, Tivantinib occupied a similar position to that in the crystal structure (Fig. 2D), whereas its orientation was reversed. Therefore, our results suggest that the diversity in structure makes it difficult to determine the binding mode of such inhibitors *in silico*, and crystal structures are necessary for structure-based drug design.

The CBSIs are a class of structurally diverse agents. Although they are all located at the colchicine binding site, different CBSIs may occupy different positions. For example, nocodazole is located deeply in the β subunit and made no interaction with α subunit (Fig. 2B). The two loops, T5 of α subunit and T7 of β subunit, cap the colchicine domain and adjust their conformation to accommodate the structurally diverse CBSIs (Fig. 1B).

The CBSIs that we report in the present study mainly bind to β-tubulin. β-tubulin isotypes have a varied distribution in different cell types and modulate the cell sensitivity to chemotherapeutic drugs [34,35]. Tumor cells may show differences in the expression of tubulin isotypes [36]. If the agents targeting tubulin could differentiate between different cell types, the undesirable side effects associated with current chemotherapeutic treatments may be reduced. It has been reported that vinblastine prefers βII-tubulin to other isotypes [37,38], providing a reason why it has good activity against leukaemia and Hodgkin's lymphoma, which express high levels of βII-tubulin. A similar situation is also reported for nocodazole [26]. In the crystal structure, C239 on βH7 is close to nocodazole (Fig. 4B). C239 in βII and βIV is substituted with S239 in βIII, with a hydroxyl group replacing the sulfhydryl group. Therefore, the nature of the residue at position 239 is most likely the main determinant of the nocodazole discrimination between tubulin isotypes. To design novel CBSIs, we may consider covalent agents that form either disulfide or ester linkage with the residue β239 to target specific β-tubulin isotypes. For example, the CBSI T138067 has been shown to bind covalently to the residue βC239 [39]. However, because T138067 binds also noncovalently to tubulin [13], it most likely targets the βIII isotype as well.

Among the ligands that we report here, nocodazole and tivantinib show activities against cancer-related kinases and microtubules, both of which are highly attractive targets for cancer chemotherapy. There is now general agreement that molecules interfering simultaneously with multiple targets might be more effective than single target agents, especially for treating complex diseases, including cancer, cardiovascular diseases, neurological diseases and metabolic diseases [40]. Targeting two pathways with one compound may increase its effectiveness and decrease drug resistance, which could be leveraged for therapeutic benefit. Compared to other microtubule interfering agents, CBSIs have owned much smaller molecular weights and simpler scaffolds, which make them excellent candidates for multitarget drug design.

To date, no CBSI has reached the commercial phase for the treatment of cancer. Our results allow us to propose a real structure-based pharmacophore for CBSIs. It will be useful for the design and improvement of CBSIs, and will also help engineer existing anti-cancer compounds to endow them with the ability to interfere with microtubules.

Materials and methods

Materials

Plinabulin (NPI-2358, Catalog # HY-14444) and Tivantinib (ARQ197, Catalog # HY-50686) were purchased from MedChemExpress (Monmouth Junction, NJ, USA). Lexibulin (CYT997, Catalog # S2195) and Nocodazole (Catalog # S2775) were obtained from Selleckchem (Houston, TX, USA). Porcine brain tubulin (Catalog # T-238P) was purchased from Cytoskeleton, Inc. (Denver, CO, USA). Bis-Tris propane, Mes, tyrosine, DTT and β,γ-methyleneadenosine 5′-triphosphate disodium salt were purchased from Sigma (St. Louis, MO, USA). β-Mercaptoethanol was obtained from XiYa Reagent (Chengdu, China). Glycerol and antiprotease cocktail were obtained from Sangon Biotech (Shanghai, China). All of the conventional reagents, such as NaCl, $MgCl_2$ and $CaCl_2$, were supplied by Kelun Pharmaceutical (Chengdu, China).

Protein expression and purification

The complex of two tubulins with the stathmin-like domain of RB3 (RB3–SLD) and with tubulin tyrosine ligase (TTL) (the T2R–TTL complex) was produced as described. In brief, RB3–SLD was overexpressed in *Escherichia coli*, purified by anion-exchange chromatography (QFF; GE Healthcare Ltd, Little Chalfont, UK) and gel filtration (Superdex 75; GE-Healthcare), concentrated to 10 $mg{\cdot}mL^{-1}$ and stored at −80 °C until use [13,41]. The TTL construct was a kind gift from Dr Michel O. Steinmetz (Paul Scherrer Institut, PSI, Switzerland). TTL was purified as described with slight modifications [42]. Briefly, after overexpression in *E. coli*, it was purified by nickel-affinity chromatography followed by gel filtration (Superdex 200; GE-Healthcare). Finally, TTL in Bis-Tris propane (pH 6.5), 200 mM NaCl, 2.5 mM $MgCl_2$, 5 mM β-mercaptoethanol and 1% glycerol was concentrated to 20 $mg{\cdot}mL^{-1}$ and stored at −80 °C. Porcine brain tubulin

(Catalog # T-238P) was supplied at 10 mg·mL^{-1} (buffer: 80 mM Pipes, pH 6.9, 2.0 mM $MgCl_2$, 0.5 mM EGTA and 1 mM GTP) and stored at −80 °C until use. The T2R–TTL complex was prepared by mixing tubulin, RB3–SLD and TTL in a 2 : 1.3 : 1.2 (tubulin : RB3–SLD : TTL) molar ratio, and then 1 mM β,γ-methyleneadenosine 5′-triphosphate disodium salt, 5 mM tyrosine and 10 mM DTT were added and the complex was concentrated to 20 mg·mL^{-1} at 4 °C.

Crystallization and crystals soaking

T2R–TTL crystals were obtained at 20 °C in a buffer consisting of 6% poly(ethylene glycol) 4000, 8% glycerol, 0.1 M Mes, 30 mM $CaCl_2$ and 30 mM $MgCl_2$ (pH 6.7). Rod-like crystals grew to maximum dimensions within 1 week. Stock solutions of ligands were prepared in 100% DMSO at 5 mM (plinabulin and lexibulin) or 10 mM (tivantinib and nocodazole) concentrations. For crystal soaking, 0.1 μL of the ligand solution was added to the 2-μL crystal-containing drop for 24 h at 20 °C.

Data collection and structure determination

The crystals of T2R–TTL–ligand complexes were mounted in nylon loops (Hampton, Aliso Viejo, CA, USA) and flash-cooled in a cold nitrogen stream at 100 K. Diffraction data were collected on beamlines BL17U1 and BL19U1 at Shanghai Synchrotron Radiation Facility (SSRF) (Shanghai, China). Data were processed using HKL2000 [43]. The structures were determined by molecular replacement method using the T2R–TTL structure [Protein Data Bank (PDB) code: 4I55] as a search model. Manual model building were performed with COOT [44]. All refinements were performed using the refinement module phenix.refine of PHENIX [45]. The initial models and the topology parameters for the ligands were generated with PRODRG [46]. The model quality was checked with MOLPROBITY [47]. PYMOL [48] was used to generate the figures.

Acknowledgements

We thank Dr Michel O.Steinmetz (Paul Scherrer Institut, PSI, Switzerland) for kindly providing the plasmid of TTL, as well as Dr Rongguang Zhang for kindly providing the beamline time on BL19U1 at SSRF. We also thank Dr Qisheng Wang and Dr Feng Yu for their skillful guidance at beamline BL17U1. John Yun-Chung Chen (University of California, Berkeley) is acknowledged for his kind help with modifying the statement. This work was supported by research funding received from National Major Scientific and Technological Special Project for 'Significant New Drugs Development' (2012ZX09103301-030), National Natural Science Foundation of China (81372822) and Scientific Research Foundation for the Returned Overseas Chinese Scholars (2014-1685-11-9), State Education Ministry.

Author contributions

YW, QC and JY participated in the research design. YW, HZ, YW, XC, QL and ZY conducted the experiments, including protein expression and purification, crystallization and crystal soaking, and data collection. QC and YY performed the data analysis. YW, BG, QC and JY wrote or contributed to the writing of the manuscript.

References

1 Kavallaris M (2010) Microtubules and resistance to tubulin-binding agents. *Nat Rev Cancer* **10**, 194–204.
2 Zhou J & Giannakakou P (2005) Targeting microtubules for cancer chemotherapy. *Curr Med Chem Anticancer Agents* **5**, 65–71.
3 Hammond JW, Cai D & Verhey KJ (2008) Tubulin modifications and their cellular functions. *Curr Opin Cell Biol* **20**, 71–76.
4 Cone NJ, Miller R & Neuss N (1963) Alkaloids of Vinca rosea Linn. (Catharanthus roseus G. Don). XV. Analysis of vinca alkaloids by thin-layer chromatography. *J Pharm Sci* **52**, 688–692.
5 Nogales E, Wolf SG, Khan IA, Luduena RF & Downing KH (1995) Structure of tubulin at 6.5 A and location of the taxol-binding site. *Nature* **375**, 424–427.
6 Gigant B, Wang C, Ravelli RB, Roussi F, Steinmetz MO, Curmi PA, Sobel A & Knossow M (2005) Structural basis for the regulation of tubulin by vinblastine. *Nature* **435**, 519–522.
7 Ravelli RB, Gigant B, Curmi PA, Jourdain I, Lachkar S, Sobel A & Knossow M (2004) Insight into tubulin regulation from a complex with colchicine and a stathmin-like domain. *Nature* **428**, 198–202.
8 Prota AE, Bargsten K, Northcote PT, Marsh M, Altmann KH, Miller JH, Diaz JF & Steinmetz MO (2014) Structural basis of microtubule stabilization by laulimalide and peloruside A. *Angew Chem Int Ed Engl* **53**, 1621–1625.
9 Prota AE, Bargsten K, Diaz JF, Marsh M, Cuevas C, Liniger M, Neuhaus C, Andreu JM, Altmann KH & Steinmetz MO (2014) A new tubulin-binding site and pharmacophore for microtubule-destabilizing anticancer drugs. *Proc Natl Acad Sci USA* **111**, 13817–13821.
10 Lu Y, Chen J, Xiao M, Li W & Miller DD (2012) An overview of tubulin inhibitors that interact with the colchicine binding site. *Pharm Res* **29**, 2943–2971.

11 Hartung EF (1954) History of the use of colchicum and related medicaments in gout; with suggestions for further research. *Ann Rheum Dis* **13**, 190–200.
12 Weisenberg RC, Borisy GG & Taylor EW (1968) The colchicine-binding protein of mammalian brain and its relation to microtubules. *Biochemistry* **7**, 4466–4479.
13 Dorleans A, Gigant B, Ravelli RB, Mailliet P, Mikol V & Knossow M (2009) Variations in the colchicine-binding domain provide insight into the structural switch of tubulin. *Proc Natl Acad Sci USA* **106**, 13775–13779.
14 Barbier P, Dorleans A, Devred F, Sanz L, Allegro D, Alfonso C, Knossow M, Peyrot V & Andreu JM (2010) Stathmin and interfacial microtubule inhibitors recognize a naturally curved conformation of tubulin dimers. *J Biol Chem* **285**, 31672–31681.
15 Prota AE, Danel F, Bachmann F, Bargsten K, Buey RM, Pohlmann J, Reinelt S, Lane H & Steinmetz MO (2014) The novel microtubule-destabilizing drug BAL27862 binds to the colchicine site of tubulin with distinct effects on microtubule organization. *J Mol Biol* **426**, 1848–1860.
16 Löwe J, Li H, Downing KH & Nogales E (2001) Refined structure of alpha beta-tubulin at 3.5 A resolution. *J Mol Biol* **313**, 1045–1057.
17 Lickliter JD, Francesconi AB, Smith G, Burge M, Coulthard A, Rose S, Griffin M, Milne R, McCarron J, Yeadon T *et al*. (2010) Phase I trial of CYT997, a novel cytotoxic and vascular-disrupting agent. *Brit J Cancer* **103**, 597–606.
18 Burge M, Francesconi AB, Kotasek D, Fida R, Smith G, Wilks A, Vasey PA & Lickliter JD (2013) Phase I, pharmacokinetic and pharmacodynamic evaluation of CYT997, an orally-bioavailable cytotoxic and vascular-disrupting agent. *Invest New Drug* **31**, 126–135.
19 Chen X, Yang C, Xu Y, Zhou H, Liu H & Qian W (2013) The microtubule depolymerizing agent CYT997 effectively kills acute myeloid leukemia cells via activation of caspases and inhibition of PI3K/Akt/mTOR pathway proteins. *Exp Ther Med* **6**, 299–304.
20 Burns CJ, Harte MF, Bu X, Fantino E, Joffe M, Sikanyika H, Su S, Tranberg CE, Wilson N, Charman SA *et al*. (2009) Discovery of CYT997: a structurally novel orally active microtubule targeting agent. *Bioorg Med Chem Lett* **19**, 4639–4642.
21 Park H, Hong S & Hong S (2012) Nocodazole is a high-affinity ligand for the cancer-related kinases ABL, c-KIT, BRAF, and MEK. *ChemMedChem* **7**, 53–56.
22 De Brabander MJ, Van de Veire RM, Aerts FE, Borgers M & Janssen PA (1976) The effects of methyl (5-(2-thienylcarbonyl)-1H-benzimidazol-2-yl) carbamate, (R 17934; NSC 238159), a new synthetic antitumoral drug interfering with microtubules, on mammalian cells cultured in vitro. *Cancer Res* **36**, 905–916.
23 Nguyen TL, McGrath C, Hermone AR, Burnett JC, Zaharevitz DW, Day BW, Wipf P, Hamel E & Gussio R (2005) A common pharmacophore for a diverse set of colchicine site inhibitors using a structure-based approach. *J Med Chem* **48**, 6107–6116.
24 Aguayo-Ortiz R, Méndez-Lucio O, Medina-Franco JL, Castillo R, Yépez-Mulia L, Hernández-Luis F & Hernández-Campos A (2013) Towards the identification of the binding site of benzimidazoles to β-tubulin of Trichinella spiralis: insights fromcomputational and experimental data. *J Mol Graph Model* **41**, 12–19.
25 Santoshi S & Naik PK (2014) Molecular insight of isotypes specific beta-tubulin interaction of tubulin heterodimer with noscapinoids. *J Comput Aid Mol Des* **28**, 751–763.
26 Xu K, Schwarz PM & Ludueña RF (2002) Interaction of nocodazole with tubulin isotypes. *Drug Develop Res* **55**, 91–96.
27 Mita MM, Spear MA, Yee LK, Mita AC, Heath EI, Papadopoulos KP, Federico KC, Reich SD, Romero O, Malburg L *et al*. (2010) Phase 1 first-in-human trial of the vascular disrupting agent plinabulin(NPI-2358) in patients with solid tumors or lymphomas. *Clin Cancer Res* **16**, 5892–5899.
28 Millward M, Mainwaring P, Mita A, Federico K, Lloyd GK, Reddinger N, Nawrocki S, Mita M & Spear MA (2012) Phase 1 study of the novel vascular disrupting agent plinabulin (NPI-2358) and docetaxel. *Invest New Drug* **30**, 1065–1073.
29 Yamazaki Y, Sumikura M, Hidaka K, Yasui H, Kiso Y, Yakushiji F & Hayashi Y (2010) Anti-microtubule 'plinabulin' chemical probe KPU-244-B3 labeled both alpha- and beta-tubulin. *Bioorg Med Chem* **18**, 3169–3174.
30 Rota Caremoli E & Labianca R (2014) Tivantinib: critical review with a focus on hepatocellular carcinoma. *Expert Opin Inv Drug* **23**, 1563–1574.
31 Kang YK, Muro K, Ryu MH, Yasui H, Nishina T, Ryoo BY, Kamiya Y, Akinaga S & Boku N (2014) A phase II trial of a selective c-Met inhibitor tivantinib (ARQ 197) monotherapy as a second- or third-line therapy in the patients with metastatic gastric cancer. *Invest New Drug* **32**, 355–361.
32 Goldman JW, Laux I, Chai F, Savage RE, Ferrari D, Garmey EG, Just RG & Rosen LS (2012) Phase 1 dose-escalation trial evaluating the combination of the selective MET (mesenchymal-epithelial transition factor) inhibitor tivantinib (ARQ 197) plus erlotinib. *Cancer* **118**, 5903–5911.
33 Aoyama A, Katayama R, Oh-Hara T, Sato S, Okuno Y & Fujita N (2014) Tivantinib (ARQ 197) exhibits antitumor activity by directly interacting with tubulin and overcomes ABC transporter-mediated drug resistance. *Mol Cancer Ther* **13**, 2978–2990.

34 Gan PP, Pasquier E & Kavallaris M (2007) Class III beta-tubulin mediates sensitivity to chemotherapeutic drugs in non small cell lung cancer. *Cancer Res* **67**, 9356–9363.
35 Gan PP & Kavallaris M (2008) Tubulin-targeted drug action: functional significance of class II and class IVb beta-tubulin in vinca alkaloid sensitivity. *Cancer Res* **68**, 9817–9824.
36 Scott CA, Walker CC, Neal DA, Harper CE, Bloodgood RA, Somers KD, Mills SE, Rebhun LI & Levine PA (1990) Beta-tubulin epitope expression in normal and malignant epithelial cells. *Arch Otolaryngol Head Neck Surg* **116**, 583–589.
37 Walss-Bass C, Kreisberg JI & Luduena RF (2003) Effect of the antitumor drug vinblastine on nuclear betaII-tubulin in cultured rat kidney mesangial cells. *Invest New Drug* **21**, 15–20.
38 Ravanbakhsh S, Gajewski M, Greiner R & Tuszynski JA (2013) Determination of the optimal tubulin isotype target as a method for the development of individualized cancer chemotherapy. *Theor Biol Med Model* **10**, 29.
39 Shan B, Medina JC, Santha E, Frankmoelle WP, Chou TC, Learned RM, Narbut MR, Stott D, Wu P, Jaen JC *et al.* (1999) Selective, covalent modification of beta-tubulin residue Cys-239 by T138067, an antitumor agent with in vivo efficacy against multidrug-resistant tumors. *Proc Natl Acad Sci USA* **96**, 5686–5691.
40 Lu JJ, Pan W, Hu YJ & Wang YT (2012) Multi-target drugs: the trend of drug research and development. *PLoS ONE* **7**, e40262.
41 Charbaut E, Curmi PA, Ozon S, Lachkar S, Redeker V & Sobel A (2001) Stathmin family proteins display specific molecular and tubulin binding properties. *J Biol Chem* **276**, 16146–16154.
42 Prota AE, Bargsten K, Zurwerra D, Field JJ, Diaz JF, Altmann KH & Steinmetz MO (2013) Molecular mechanism of action of microtubule-stabilizing anticancer agents. *Science* **339**, 587–590.
43 Otwinowski Z & Minor W (1997) Processing of X-ray diffraction data collected in oscillation mode. *Macromol Crystallogr A* **276**, 307–326.
44 Emsley P & Cowtan K (2004) Coot: model-building tools for molecular graphics. *Acta Crystallogr D Biol Crystallogr* **60**, 2126–2132.
45 Adams PD, Grosse-Kunstleve RW, Hung LW, Ioerger TR, McCoy AJ, Moriarty NW, Read RJ, Sacchettini JC, Sauter NK & Terwilliger TC (2002) PHENIX: building new software for automated crystallographic structure determination. *Acta Crystallogr D Biol Crystallogr* **58**, 1948–1954.
46 Schuttelkopf AW & van Aalten DM (2004) PRODRG: a tool for high-throughput crystallography of protein-ligand complexes. *Acta Crystallogr D Biol Crystallogr* **60**, 1355–1363.
47 Chen VB, Arendall WB, Headd JJ, Keedy DA, Immormino RM, Kapral GJ, Murray LW, Richardson JS & Richardson DC (2010) MolProbity: all-atom structure validation for macromolecular crystallography. *Acta Crystallogr D Biol Crystallogr* **66**, 12–21.
48 DeLano WL (2002) The PyMOL Molecular Graphics System. http://www.pymol.org.